

Nickel Nanoparticles on Carbon Nanotubes: Synthesis, Characterization and Hydrogen Storage

M.Z. Figueroa-Torres^{1,*}, C. Dominguez-Rios¹, J.G. Cabanas-Moreno², K. Suarez-Alcantara² and A. Aguilar-Elguezabal^{1,†}

¹Centro de Investigación en Materiales Avanzados, S. C., Depto. de Química de Materiales. Miguel de Cervantes 120, Complejo Industrial Chihuahua, CP. 31130, Chihuahua, Chihuahua, México.

²Instituto Politécnico Nacional, UPALM, Escuela Superior de Física y Matemáticas, Departamento de Ciencia de Materiales, Apdo. Postal 21-408, C.P. 04021, México, DF, México

Received: November 18, 2009, Accepted: January 26, 2010

Abstract: Nickel nanoparticles were deposited on multiwall carbon nanotubes (Ni-MWCNT) in a single step by electroless plating technique. The effect of bath composition on the resulting nanoparticles was examined by scanning and transmission electron microscopy. To improve nickel dispersion a surface treatment was made to raw MWCNT. Hydrogen storage measurements were determined at 77 K and atmospheric pressure and also at 303 K in the pressure range of 0.1 to 5 MPa. Results show that highly dispersed nickel nanoparticles were deposited on the external MWCNT wall using hydrazine as reducing agent. Surface modifications help to improve hydrogen storage. For Ni-MWCNT hydrogen storage was increased two times compared to raw MWCNT at 303 K and 5 MPa.

Keywords: Carbon Nanotubes, nickel, electroless, Hydrogen storage

1. INTRODUCTION

Development and implementation of environmentally friendly fuels is a topic of great interest. Hydrogen is the ideal energy carrier especially for mobile applications. However, the bottleneck toward a hydrogen economy is the lack of an efficient and safe hydrogen storage medium [1]. Carbon nanostructures are a promising alternative to store hydrogen because their low density, good chemical stability and fast adsorption/desorption cycling [2-4]. Particularly, it has been proposed that hydrogen can be stored in carbon nanotubes at the exterior of the tube wall and inside the tube [1]. Lately, some works have shown that the presence of certain metals like Pt, Pd, Ti, V, Co, Ni, etc., improves hydrogen storage of carbon materials via spillover effect [6-12]. The advantage of hydrogen spillover is that it not only improves hydrogen storage capacity, but also increases initial hydrogen adsorption kinetics [3-6]. Ni-carbon nanotubes systems have not receive much attention and hydrogen storage capacities of such system are poorly understood. For a good hydrogen spillover effect it is crucial that metal nanoparticles are in the exterior wall of the nano-

tubes and the contact between CNT surface and metal particles must be of around 12 atoms, all this factors may be tuned by the synthesis conditions [6,7,9,10].

Conventional experimental techniques to prepare metal-CNT materials are ball-milling, wet impregnation, condensed-phase reduction, microemulsion and sputtering [6-10]. Results show that experimentally, it is difficult to obtain very small metal nanoparticles highly dispersed on the MWCNT surface and some of the above mentioned methods induce the destruction of the intrinsic nanotubes structure [6-10].

In this paper, we describe the synthesis of MWCNT containing disperse nickel nanoparticles by adapting electroless plating technique. We report the hydrogen storage capacity of Ni doped MWCNT at 77 K and atmospheric pressure and also at 303 K and a pressure range of 0.1-5 MPa and are compared to the raw MWCNT.

2. EXPERIMENTAL

2.1. Synthesis of MWCNT

MWCNT have been synthesized by the pyrolysis of hydrocarbon and ferrocene mixture inside a quartz tube heated by a cylindrical furnace at a constant temperature of 1073 K. Toluene and

To whom correspondence should be addressed:
Email: *m_zyzlila@yahoo.com.mx †alfredo.aguilar@cimav.edu.mx
Phone: Tel +52 614 4394820; fax: +52 614 4391130

acrylonitrile were used as carbon source being nitrogen a dopant for the synthesis with acrylonitrile. In the first case, 0.75 g of ferrocene were dissolved in 20 mL of toluene and in the second case 0.1 g of ferrocene were dissolved in 20 mL of acrylonitrile. The mixture was fed using an argon flow of 1 L/min.

2.2. Activation of MWCNT surface

In order to modify MWCNT surface, they were chemically activated with KOH. The ratio of KOH and MWCNT was fixed at 4:1 (g/g). Activation was done under 150 cm³/min of nitrogen flow at 1073 K for 30 min. To remove all the solid products of the activation reaction, activated nanotubes were washed with HCl (5M) and then with HNO₃ (3M) and finally rinsed several times with distilled water. Samples were dried at 383 K during 8 h.

2.3. Preparation and characterization of Ni-MWCNT.

MWCNT were doped with nickel by electroless plating technique. Two different electroless plating baths have been studied; both of them were originally designed for the plating of metallic surfaces [13,14], so the process was slightly modified to favor the deposit on the MWCNT walls. The composition of the electroless plating baths and the processing parameters are listed in Table 1.

Electroless baths were prepared from analytical grade chemicals and distilled water in a beaker. Electroless plating was made on a hot plate with a magnetic stirrer. Before plating treatment MWCNT were placed in the electroless bath and ultrasonically dispersed. After nickel deposition, MWCNT were separated from the solution by filtration and then rinsed several times with distilled water and dried at 383 K for 8 h.

Morphologies of samples were studied using a Jeol JSM-7401 scanning electron microscope (SEM) adapted with energy dispersive spectrometry system (EDS) for chemical analysis. Some images were obtained by transmission electron microscopy (TEM) Philips model CM-200, equipped with EDS Prime. X-Ray spectroscopy was useful to characterize the nickel nanoparticles.

To evaluate the surface area of the samples, physical adsorption of N₂ at 77 K was carried out in an automatic gas sorption analyzer (Quantachrome Autosorb 1). Before measurements, samples were outgassed at 573 K for 3 h. Surface area (A_{BET}) was obtained using the multipoint BET method.

2.4. Hydrogen storage evaluation

Hydrogen adsorption at 77 K and atmospheric pressure were measured in a standard volumetric apparatus (Quantachrome Autosorb 1). The hydrogen adsorption capacity was determined using

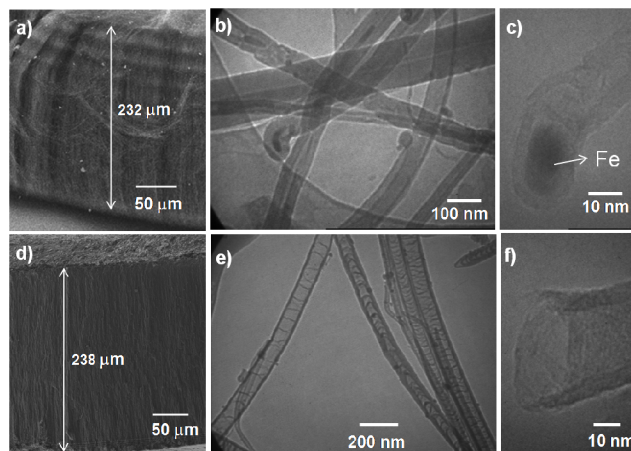


Figure 1. MWCNT's Micrographs. a) toluene MWCNT's on quartz tube; b) and c) TEM images; d) acrylonitrile MWCNT's on quartz tube; e) and f) TEM images.

the value of the adsorbed volume at 0.995 P/P₀ and the ideal gas equation. The value of 0.995 P/P₀ is very close to the value of the atmospheric pressure. Before measurements, the samples were degassed in vacuum at 573 K for 3 h.

Hydrogen adsorption at 303 K and pressures from 0.1 to 5 MPa were evaluated using a high pressure gravimetric analyzer equipped with a magnetic levitation microbalance PCTM-6000 from Techno System CO, LTD. To avoid all traces of condensable vapors that might affect gravimetric measurements ultra high purity hydrogen was used. Before each analysis, samples were degassed for 2 h at 673 K. The sample weight for each analysis was fixed at 1 g.

3. RESULTS AND DISCUSSIONS

Figure 1 shows the morphology of the MWCNT synthesized with toluene (Figure 1a, 1b and 1c) and acrylonitrile (figure 1d, 1e, 1f). MWCNT grow perpendicularly on the inner surface of quartz tube used as substrate and have an approximate length of 230 mm. Their external diameter varies from 30 to 80 nm.

The main difference between nanotubes synthesized using toluene and acrylonitrile is the number of internal walls. As can be appreciated in figure 1b, toluene nanotubes have many internal walls, so inner diameter is small and almost all the internal chan-

Table 1. Components, concentrations and experimental conditions of electroless plating baths.

	DMAB based bath		Hydrazine based bath	
Ni precursor (g/L)	NiSO ₄ ·6H ₂ O	57.6	Ni(C ₂ H ₃ O ₂) ₂ ·4H ₂ O	29.86
Complexing agent (g/L)	Na ₃ (citrate)	44	Na ₂ EDTA ⁺	5.96
Stabilizer (g/L)	2MBT*	0.0125	Lactic acid	13.51
Reducing agent (g/L)	DMAB**	23.6	Hydrazine	12.82
			NaOH	7.5
Processing parameters	pH	6		9.6
	Temperature	333-353 K		333-353 K
	Immersion time	5-60 min		5-30 min

*2Mercaptobenzothiazol. **Dimethylamine-borane complex. ⁺ Na Ethylenediamine tetraacetic acid

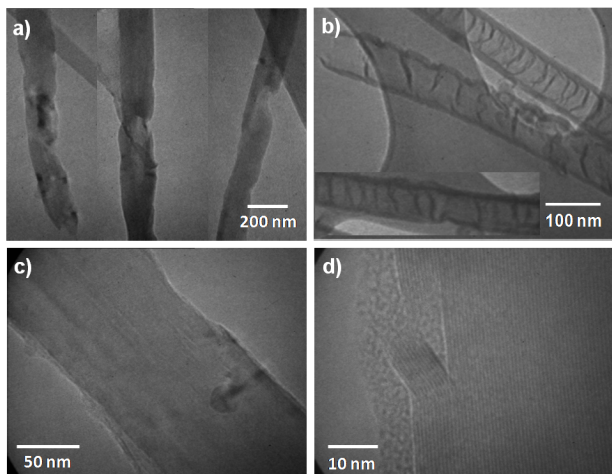


Figure 2. TEM images of MWCNT after chemical activation with KOH a) and c) synthesized from toluene; b) and d) synthesized from acrylonitrile.

nels are blocked by metallic iron particles formed from ferrocene to induce the formation of MWCNT. Otherwise, acrylonitrile nanotubes present few internal walls, the thickness of these walls is approximately 15 nm and consequently its internal diameter is large, around 70 nm. This characteristic is not common in the conventional MWCNT synthesized with sources of carbon like hexane, benzene or toluene, which are the typical hydrocarbons used. For MWCNT synthesized with acrylonitrile the internal channels are not blocked by iron particles, since most of these atoms are on the external walls (dark round particles in figure 1e).

Figure 2 illustrate morphology of the MWCNT after chemical activation with KOH. Many superficial defects were generated on the nanotubes walls, some layers of the external walls were eliminated leaving holes, even that, the nanotubular morphology was preserved. These defects are formed by carbonaceous gasification [15].

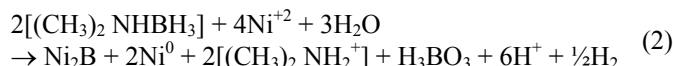
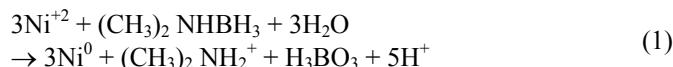
As can be seen from the figure 2, the chemical treatments removed iron particles from MWCNT and for toluene CNT opened mouth of channels can be appreciated. Main residual iron is placed deep inside in the channels of nanotubes made from toluene, which are inaccessible sites for the HCl and HNO₃.

3.1. Ni deposition on MWCNT

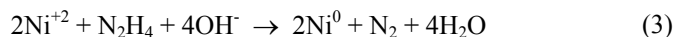
First experiments were made using raw MWCNT, in those conditions, nickel is not deposited on the MWCNT even several temperatures and immersion times were experimented. In the technical articles where nickel is deposited by electroless, authors have reported the use of a sensitization-activation step to functionalize the

surface [16-18]. Conventionally, palladium atoms are deposited on substrate by a sequence of sensitizing with SnCl₂ solution and treatment with PdCl₂ solution. The Pd atoms act as seeds, starting thus the electroless deposition of nickel. In our case, for activated MWCNT sensitization-activation step was not necessary to deposit nickel, main difference between raw and activated MWCNT is the OH- group attached to the walls, consequently, the success on the deposit of metallic nickel on the activated MWCNT seems to be dependent of the OH- groups generated during the activation process. These attached OH- groups react with nickel ions (Ni²⁺) of the bath forming a nickel hydroxide bonded to MWCNT external wall. Next, nickel hydroxide is then reduced by the ions provided by the reducing agent (DMAB or hydrazine), forming thus the nickel seed for the subsequent formation of nickel nanoparticles, nanoparticles of nickel moves on surface to form agglomerates and if immersion time is enough, nickel agglomerates grow up until the formation of a nickel film on the external wall, see figure 3.

The electroless plating mechanism for both bath formulation (DMAB and hydrazine) is similar, being the main difference the co-deposition of bore for the use of DMAB. The formation of a plating layer on the external surface of particles is given for bath conditions where deposition rate is higher than the diffusion rate of chemical species to the internal porosity of particles. The deposit obtained when DMAB is used for metals plating, is metallic nickel and Ni-B alloy. DMAB reduction reaction involves the formation of H₃BO₃ and the release of three hydride ions (H⁻), which deliver the electron pair to reduce nickel ions. The reduction of the Ni²⁺ with DMAB can be described with the following equations [13]:



For hydrazine based bath pure metallic nickel is obtained. In the process, hydrazine is oxidized to give only N₂ and water. The global equation for the reduction of the Ni²⁺ is [13]:



Reaction (3) explains the high efficiency of hydrazine as reducing agent since it is directly involved in the reduction of the Ni²⁺ without intermediary species.

3.2. Characterization of Ni-MWCNT

For DMAB based bath it was observed that when immersion time is lower than 5 minutes deposition of Ni was negligible for all tested temperatures (353 K, 343 K ó 333 K). The first Ni seeds were deposited between 7 and 10 minutes of immersion time, and after that, deposition rate increased considerably and in only 3 minutes more, a film is formed around MWCNT. This fast increase in

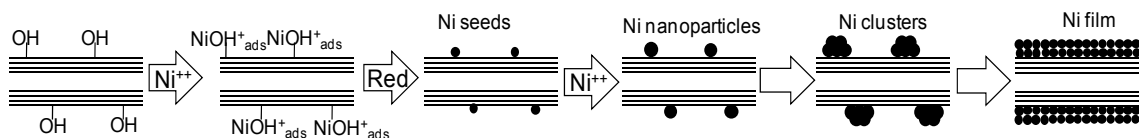


Figure 3. Steps of nickel formation by electroless in MWCNT.

deposition rate is due to the autocatalytic nature of electroless reactions, i.e., nickel is continuously deposited and the depositing process will not stop until Ni^{2+} ions are totally consumed or reducing agent become unavailable. Figure 4 shows Ni-MWCNT prepared with DMAB bath.

Figure 4b shows MWCNT completely recovered with nickel. Observation at higher magnifications reveals that nickel grow up around external wall of nanotubes forming big spheres, but, there are too some places where only a small film of nickel is formed and nickel film blocks the access to the internal channels of carbon nanotubes (figure 4d). In order to control deposition rate and thus obtain only highly dispersed nickel nanoparticles, deposition temperature were reduced to 343 K, however, the obtained results were the same as for 353 K. When temperature was decrease to 333 K experiments did not show nickel deposition below one hour of immersion time, this could be because the activation energy to form nickel seed is so high and under this temperature the energy barrier cannot be surpassed.

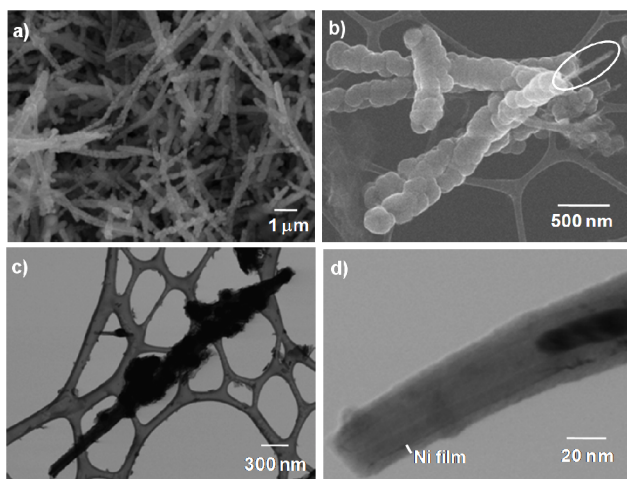


Figure 4. Images of Ni-MWCNT using DMAB bath at 353 K and immersion time of 15 minutes. a) and b) SEM images; c) and d) TEM images

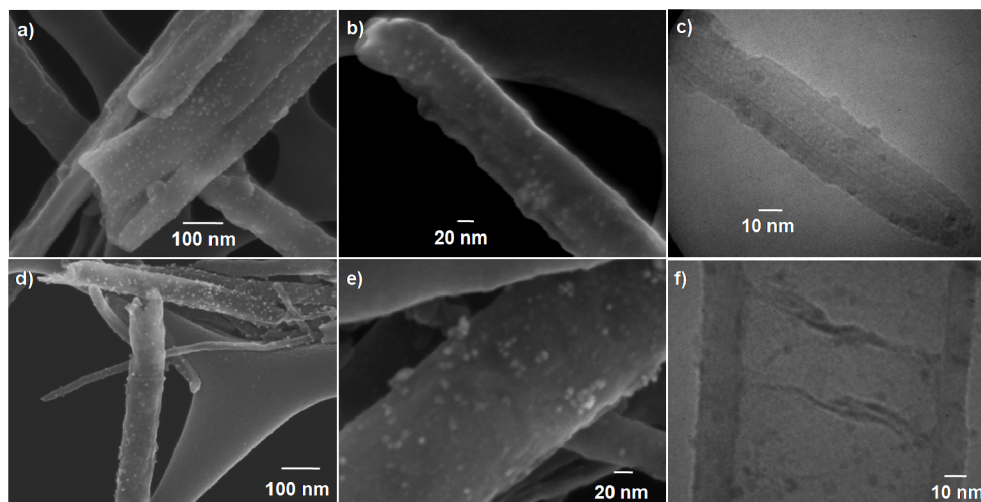


Figure 5. Images of Ni-MWCNT using hydrazine bath at 333 K and immersion time of 15 minutes, a), b), c) MWCNT synthesized from toluene; d), e), f) MWCNT synthesized from acrylonitrile.

Figure 5 shows Ni-MWCNT prepared using hydrazine based bath at 333 K, only nickel nanoparticles randomly dispersed are observed although long plating times were used.

As can be seen, with the use of hydrazine a very good dispersion of nickel nanoparticles was obtained in both kinds of carbon nanotubes; the particles presented spherical shape and particle size is in the range of 3-8 nm. Zubizarreta et al. [19] doped carbon nanospheres with nickel using impregnation technique, they obtained Ni agglomerates of around 20 nm and dispersion was poor for Ni contents higher than 5 wt. %. Rather et al. [10] prepared Pd-MWCNT by in situ condensed phase reduction method; their results show that most of the particles are confined in the interior of the carbon nanotubes channels. In our case, all Ni nanoparticles are attached to the external wall of carbon nanotubes.

3.3. Hydrogen storage

BET surface area (A_{BET}) and hydrogen storage capacity measured at 77K and atmospheric pressure of raw MWCNT, activated MWCNT and Ni/MWCNT are reported in table 2.

BET surface area of toluene raw MWCNT is 25 m^2/g and for acrylonitrile is almost twice. For both types of nanotubes, after activation treatment the BET surface area increases considerably as well as hydrogen storage capacity. This increment is attributed to the surface defects generated by the chemical activation process; since these defects are preferential places for hydrogen adsorption [20]. Nevertheless, hydrogen storage quantity is low and it is not attractive for practical applications. It is also appreciated that there

Table 2. BET surface area and Hydrogen storage at 77 K and atmospheric pressure.

	Treatment	A_{BET} (m^2/g)	wt. % H_2
MWCNT synthesized from toluene	Raw	25	0.04
	Activated	48	0.12
	Act. with Ni	52	0.15
MWCNT synthesized from acrylonitrile	Raw	49	0.05
	Activated	144	0.16
	Act. with Ni	145	0.17

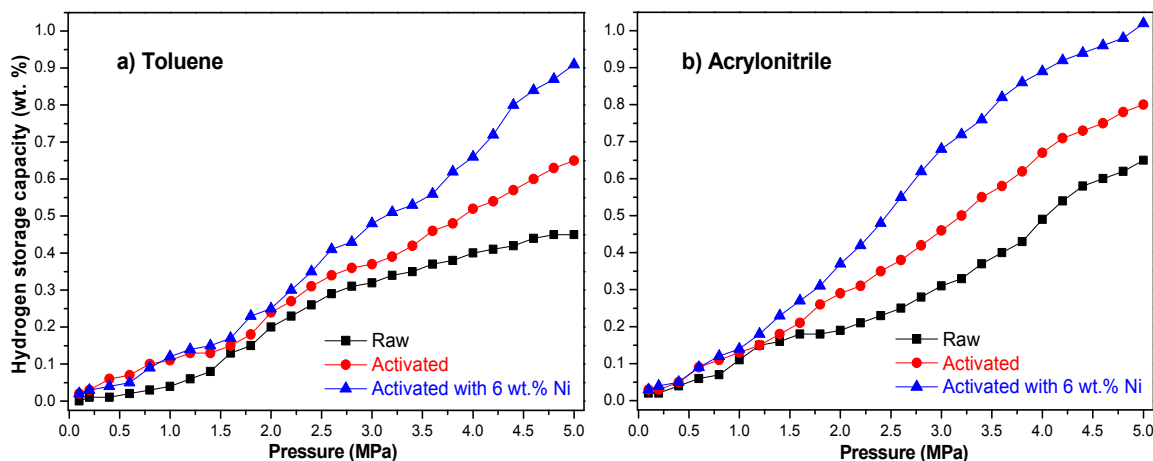


Figure 6. Hydrogen storage capacity at 303 K and different pressures.

is not an increase in hydrogen storage with nickel dispersion; this is because the measured conditions are not adequate for spillover phenomena, therefore hydrogen storage is present only by physisorption. High pressure hydrogen isotherms at 303 K for raw, activated and Ni-MWCNT are presented in figure 6.

Figures show that hydrogen storage is a lineal function of the applied pressure, from the isotherms can be appreciated that at 5 MPa samples have not yet been saturated, suggesting that if we continue increasing pressure hydrogen storage will increase. For both types of nanotubes at pressures less than 1.5 MPa doesn't exist great difference between the quantities of hydrogen adsorbed, considerable differences appear at pressures higher than 2 MPa.

In raw and activated carbon nanotubes hydrogen adsorption is only given by physisorption and the formation of a monolayer promoted by the pressure is presented, activated CNTs shown higher hydrogen adsorption capacity than the raw due to the superficial defects, which increase the BET surface area and carboxyl groups anchored to the surface favor the hydrogen adsorption [21]. Activated toluene's CNTs at 5 MPa adsorb 0.64 H₂ wt. %, this is 1.45 times more than the raw, while, activated CNTs obtained from acrylonitrile adsorb 0.8 wt. % which is 1.2 times more compared with the raw CNTs.

By doping MWCNT with 6 wt % of nickel, hydrogen adsorption increase notably, as shown in figure 6. The maximum hydrogen storage capacity was 0.92 wt. % for toluene and 1.03 wt. % for acrylonitrile CNTs. In comparison with raw nanotubes hydrogen adsorption has been enhanced by a factor of 2. This increase in the hydrogen storage capacity cannot be attributed to different nature of surface or available surface area of raw CNTs vs. Ni-MWCNT and neither to the geometrical surface exposed by nickel nanoparticles. Even assuming 100 % dispersion of Ni on MWCNT and that one atomic hydrogen is absorbed by one nickel atom; for 6 wt. % of Ni, nickel itself will adsorb only 0.03 wt % of hydrogen, so, if individual contributions of nickel and the MWCNT were considered additive, the expected hydrogen storage capacity of the Ni-MWCNT would be slightly greater than raw-MWCNT. Therefore, enhancement in the hydrogen storage capacity was clear evidence of spillover of atomic hydrogen from Ni nanoparticles to the

MWCNT receptor [5-11]. This enhance is also related to the high dispersion of nickel nanoparticles obtained by electroless plating technique, since nanoparticles are small and exist an excellent contact between these nanoparticles and CNTs surface, hydrogen spillover is promoted. This result agrees with Lachawiec's report [22], they found that improving the contact between metal and carbon material the hydrogen storage capacity increase to double or triple.

Comparing our results, the hydrogen storage capacity of Ni-MWCNT prepared by the one step electroless deposition method reported here, is equivalent or superior to the capacity reported in others studies under similar measurement conditions for carbon nanotubes or spheres, using others metals and different techniques of synthesis [19-25]. Zubizarreta et al. [19] found and hydrogen storage of 0.22 wt.% at 5 MPa for Ni-doped carbon nanospheres. Likewise, Zacharia et al. [23] have obtained an adsorption capacity of 0.53 wt.% for Pd-MWCNT and 0.69 wt.% for V-MWCNT at 2MPa. For B-MWCNT, Sankaran et al. [24] obtained a hydrogen capacity of 0.7 wt% at 5MPa. Recently, a hydrogen storage capacity of 0.4 wt% at 1.8 MPa for TiO₂-MWCNT has been reported [25].

4. CONCLUSIONS

Results show that electroless plating technique is a viable and simple route to prepare Ni-MWCTN nanocomposites in a single step. Highly dispersed nickel nanoparticles of 3 to 8 nm were deposited on the external wall of MWCNT when hydrazine-based bath is used. Hydrogen storage is enhanced by surface defects on the external wall of MWCNT and nickel dispersion by a factor of two compared to the raw nanotubes. Ni-MWCNT synthesized with acrylonitrile present the best performance for hydrogen storage due to that the internal surface is available and molecules can diffuse easily into the channels.

5. ACKNOWLEDGMENT

To CONACYT for the financial support through the project 4777 No. 47776, to Roal Torres and Manuel Román from CIMAV for their help in the experimental part.

REFERENCES

- [1] Louis Schlapbahr and Andreas Züttler. *Nature*, 414, 353 (2001).
- [2] Yuda Yürüm, Alpay Taralp, T. Nejat Veziroglu. *Int. J. Hydrogen Energ.*, 34, 3784 (2009).
- [3] Elena David. *J. Mater. Process. Tech.* 162, 169 (2005).
- [4] R. Ströbel, J. Garche, P.T. Moseley, L. Jörissen, G. Wolf. *J. Power Sources*, 159, 781 (2006).
- [5] Lueking A, Yang R.T., *J. Catal.*, 206, 165 (2002).
- [6] Yildirim T, Ciraci S. *Phys. Rev. Lett.*, 94, 175501 (2005).
- [7] Zacharia R, Rather S-U, Hwang SW, Nahm KS. *Chem. Phys. Lett.*, 286, 434 (2007).
- [8] Lueking A, Yang RT. *AIChE J.*, 49, 1556 (2003).
- [9] M. Zielinski, R.Wojcieszak, S. Monteverdi, M. Mercy, M.M. Bettahar *Int. J. Hydrogen Energ.*, 32, 1024 (2007).
- [10]Sami-ullah Rather, Renju Zacharia, Sang Woon Hwang, Meharj-ud-din Naik, Kee Suk Nahm. *Chem. Phys. Lett.*, 441, 261 (2007).
- [11]Hyun-Seok Kim, Ho Lee, Kyu-Sung Han, Jin-Ho Kim, Min-Sang Song, Min-Sik Park, Jai-Young Lee, and Jeung-Ku Kang. *J. Phys. Chem. B*, 109, 8983 (2005).
- [12]Angela Lueking and Ralph T. Yang. *J. Catal.*, 206, 165 (2002).
- [13]G.O. Mallory, J.B. Hajdu. *Electroless Plating: Fundamentals and Applications*, American Electroplaters and Surface Finishers Society (AESF), N. Y. 1990.
- [14]S. Haag, M. Burgard, B. Ernst. *Surf. Coat. Tech.*, 201, 2166 (2006).
- [15]E. Raymundo-Piñero , D. Cazorla-Amorós, A. Linares-Solano, S. Delpeux, E. Frackowiak , K. Szostak , F. Béguin. *Carbon*, 40, 1614 (2002).
- [16]F.Z. Kong, X.B. Zhang, W.Q. Xiong, F. Liu, W.Z. Huang, Y.L. Sun, J.P. Tu, X.W. Chen. *Surf. Coat. Tech.*, 155, 33 (2002).
- [17]Li-Ming Ang, T.S. Andy Hor, Guo-Qin Xu, Chih-hang Tung, Siping Zhao, and John L.S. Wang. *Chem. Mater.*, 11, 2115 (1999).
- [18]Haijun Zhang, Xiangwei Wu, Quanli Jia, Xiaolin Jia. *Mater. Des.*, 28, 1360 (2007).
- [19]L. Zubizarreta, J.A. Menéndez, J.J. Pis, A. Arenilla. *Int. J. Hydrogen Energ.*, 24, 3070 (2009).
- [20]Peng-Xiang Hou, Shi-Tao Xu, Zhe Ying, Quan-Hong Yang, C. Liu, Hui-Ming Cheng. *Carbon*, 41, 2471 (2003).
- [21]Lifeng Wang, Frances H. Yang and Ralph T. Yang, *Ind. Eng. Chem. Res.* 48 (2009) 2920.
- [22]Anthony J. Lachawiec, Jr., Gongshing Qi, and Ralph T. Yang. *Langmuir*, 21, 11418 (2005).
- [23]Renju Zacharia, Keun Young Kim, A.K.M. Fazle Kibria, Kee Suk Nahm. *Chem. Phys. Lett.*, 412, 369 (2005).
- [24]M. Sankaran, B. Viswanathan. *Carbon*, 45, 1628 (2007).
- [25]Sami-ullah Rather, Naik Mehraj-ud-din, Renju Zacharia, Sang Wood Hwang, Ae Rahn Ki, Kee Suk Nahm. *Int. J. Hydrogen Energ.*, 34, 961 (2009).